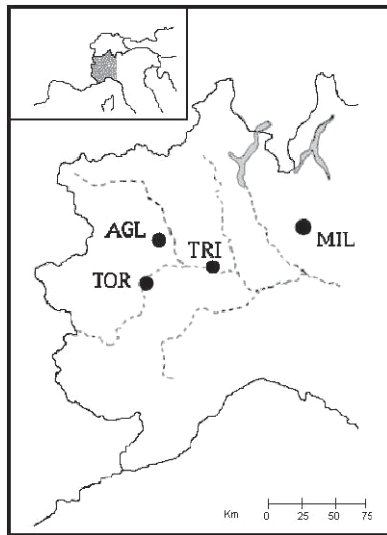


## A RAIN EPISODE RELATED TO A MESOSCALE GRAVITY WAVE

BY R. RICHIARDONE AND M. MANFRIN

**D**uring the MAP (Mesoscale Alpine Programme) experiment, the University of Turin deployed a microbarometric network and a high-precision pluviometer in the western part of the Po valley of Italy (Fig. 1). On 20 October 1999, the wave activity across the network began to increase. The following day, 21 October, the activity increased further between 0500 and 1100 UTC, coinciding (Fig. 2) with the period of maximum precipitation at Trino Vercellese (TRI). Variations of the rain rate with a period of about 1 h were also observed.



**FIG. 1.** Map of the western part of the Po valley (Italy) showing geographic placement of instruments: three-microbarometer array and a high-precision pluviometer at Trino Vercellese (TRI), three-microbarometer array in Torino (TOR), one microbarometer in Aglié (AGL), and radiosoundings in Milano (MIL).

respectively. Analysis of the time delays between pressure records in the TRI microbarometric stations

Spectral analysis of raw data during this 6-h interval showed that significant peaks, with periods of  $(66 \pm 3)$  and  $(64 \pm 3)$  min, dominated the pressure and rain spectra,

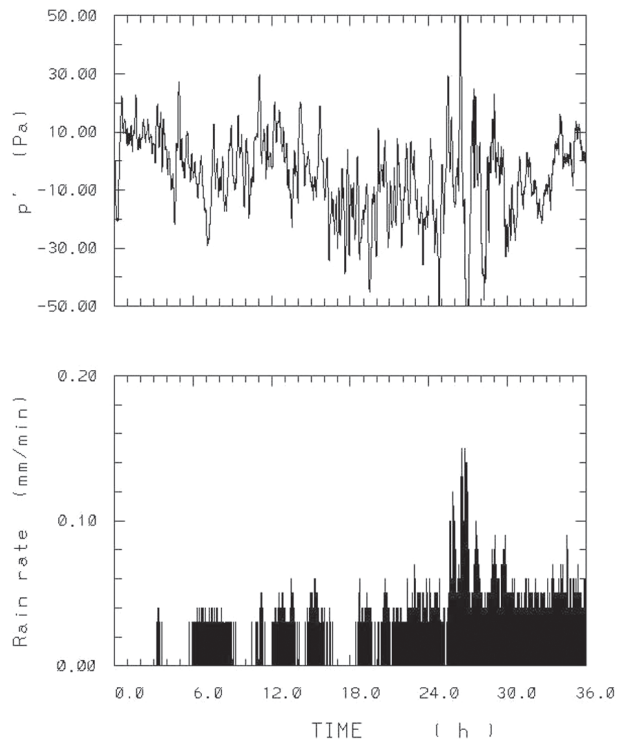


**FIG. 2.** Time series (raw data) of pressure fluctuations and rain rate between 0500 UTC on 20 Oct 1999 and 1700 UTC on 21 Oct 1999 in one of the TRI stations.

showed that the pressure peak was the signature of a gravity wave that traveled northward with a phase speed of about  $25 \text{ m s}^{-1}$  and a wavelength of about 100 km. The signature progressively decreased going westward.

A cross-correlation analysis during the period of maximum intensity of precipitation pointed out a significant correlation for about 4 h between rain rate and pressure, the rain increase following the pressure rise with a 15-min lag (i.e., about one-quarter of a period). The rain rate appeared therefore strongly coupled with the pressure fluctuations, suggesting the influence of the wave on precipitation [pressure disturbances due to the evaporative cooling can be excluded: the lowest 3 km was saturated over water

**AFFILIATION:** RICHIARDONE AND MANFRIN—Dipartimento di Fisica Generale, Università di Torino, Torino, Italy  
**CORRESPONDING AUTHOR:** R. Richiardone, Dipartimento di Fisica Generale, Università di Torino, Via P. Giuria 1, 10125, Torino, Italy  
 E-mail: richiardone@ph.unito.it

©2003 American Meteorological Society

(Fig. 3a), with saturation over ice extending up to 9 km].

Gravity-wave disturbances are often responsible for the periodic variations in rain intensity observed in many case studies. A wave conceptual model by Eom (1975) has been widely applied to explain how a gravity wave can influence precipitation. In this model, the wave is trapped (no tilt of phase lines with respect to height), and the rising and sinking motions modulate the condensation. The greatest precipitation rate follows the maximum upward motion after a certain delay in which the drops condense and fall (Fig. 4a). The wave doesn't influence the fall speed of the precipitating particles.

In this episode, the lag between the rain rate and pressure was much greater than usually observed (precipitation bands typically form between the updraft and the wave ridge). This could be explained either by Eom's model (untilted wave) in the presence of a long fall time of the precipitating particles, or by a strong upstream tilted wave (Fig. 4b). On this subject, it must be pointed out that the freezing layer was at about 2.7 km above the ground, implying that a large fraction of the falling time was spent by the particles during their solid phase [i.e., at low fall speeds (0.5–1.0 m s<sup>-1</sup>)]. Another factor that must be considered is the background wind. The wind doesn't modify the mean fall time of the precipitation particles, but it influences the lag. In the extreme case of a constant wind speed equal to the wave phase speed, the precipitation particles conserve the same

phase relationship with the wave as they fall.

A quantitative assessment of the time for the precipitation to fall is beyond the scope of this brief article. Nevertheless, by supposing that maximum condensation occurred between 4 and 6 km above ground, a rough estimate of the fall time can be made. It indicates that the observed lag, although large, is not incompatible with Eom's model prediction.

Many mechanisms can be energy sources for gravity waves, but shear instability and geostrophic adjustment were the most plausible sources for mesoscale waves discussed by Uccellini and Koch (1987). A model proposed in that paper requires both a synoptic-scale setting for wave generation and a mechanism that prevents energy loss and assures that the wave is maintained for many cycles. The generation mechanism is thought to be the geostrophic adjustment process (without excluding the shear instability) occurring in an environment characterized by the approach of an upper-level jet in a highly diffluent flow pattern, and north of a warm or stationary front at the surface (Fig. 5a).

The maintenance mechanism is wave ducting, which confines the wave propagation to horizontal, preventing energy loss due to vertical leakage. Mesoscale wave ducting requires the presence of a stable lower layer of sufficient

depth beneath a reflecting layer wherein the Richardson number is less than 0.25. This capping layer effectively reflects the vertically propagating

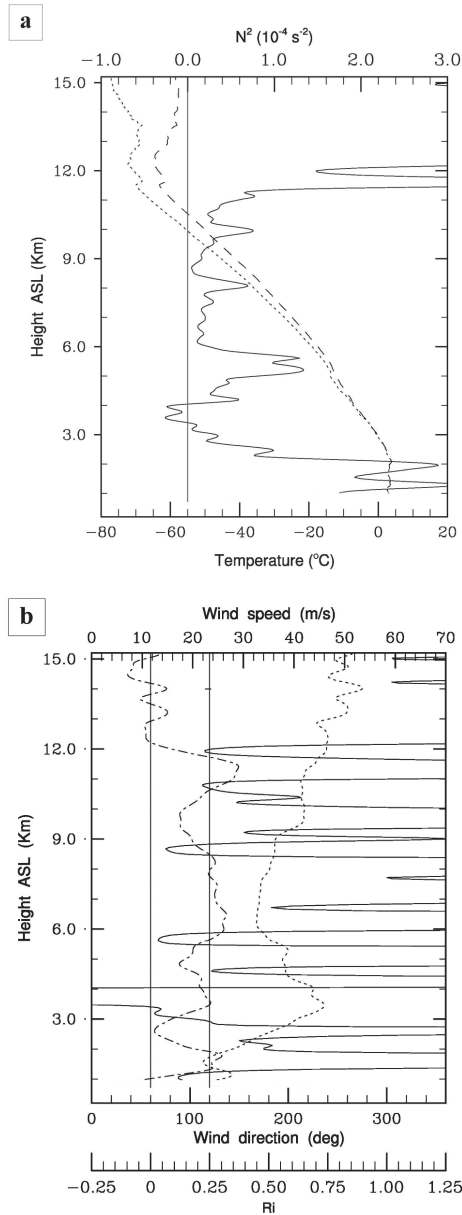


**FIG. 3. Milano (MIL) sounding at 0600 UTC on 21 Oct 1999 (running-average smoothed profiles): (a) Temperature (dashed line), dew temperature (dotted line), and the square of Brunt-Väisälä frequency  $N^2$  (moist below 9 km, dry above: solid line); vertical solid line indicates  $N^2 = 0$ ; (b) wind speed (dashed line), wind direction (dotted line), and Richardson number (solid line); vertical solid lines indicate  $Ri = 0$  and  $Ri = 0.25$ .**

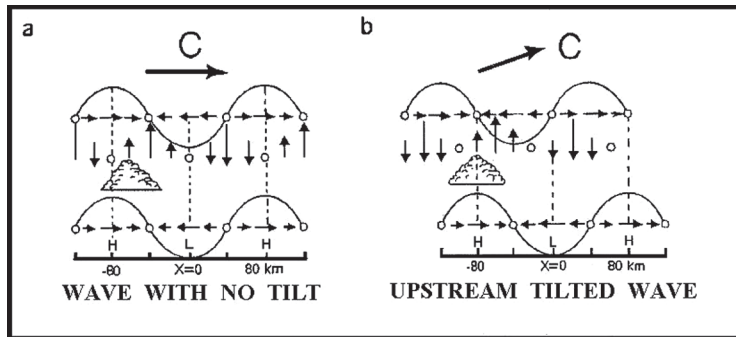


**FIG. 4.** Height variation in the phase relations between the horizontal wind component in the direction of wave propagation and the wave-induced vertical motion for (a) a gravity wave displaying no vertical tilt (Eom's model) and (b) an upstream tilted wave. The big arrow indicates the direction of propagation. Also shown is the location of maximum cloudiness relative to the gravity wave, occurring a little later than maximum vertical velocity. H and L refer to high- and low-pressure surface perturbations (after Koch and Siedlarz 1999).

waves, thus creating a duct wherein the waves may propagate horizontally without great loss of energy and need for energetic forcing. Frequently a stable layer is present near the ground ahead of a warm or occluded front; this layer is also favorable for microbarometric detection of the waves.

Unstable sheared layers (with Richardson number  $< 0.25$  including negative values), in which the flow speed in the direction of horizontal wave propagation comes very close to the phase speed of the ducted wave, are very good reflectors. In some circumstances, overreflection can occur when the wave extracts energy from the mean flow. In theory, such waves could last indefinitely. In reality, however, the environmental conditions are never homogeneous along the wave's path, so the wave would be dissipated when it moves to a region where it is no longer able to extract energy from the mean flow.

The synoptic environment on 20 and 21 October 1999 was similar to that suggested by Uccellini and Koch. The 300-hPa analysis at 1200 UTC on 20 October (Fig. 5b) looks very similar to the Uccellini and Koch conceptual model (Fig. 5a). Early on 21 October 1999, the well-defined upper-

level trough moved eastward from Spain to Sardinia, where a cut-off low developed. At the surface, a frontal system advanced from Spain (Fig. 6a) to France (Fig. 6b) during the latter half of 20 October. The system was comprised of three fronts: an occluded front toward the north, a warm front extending eastward over the Appennines, and a cold front extending southward over the Balearic Islands. During the middle of the day on 20 October, moderate, stratiform precipitation started at Trino Vercellese, at first irregularly and then, after midnight, con-

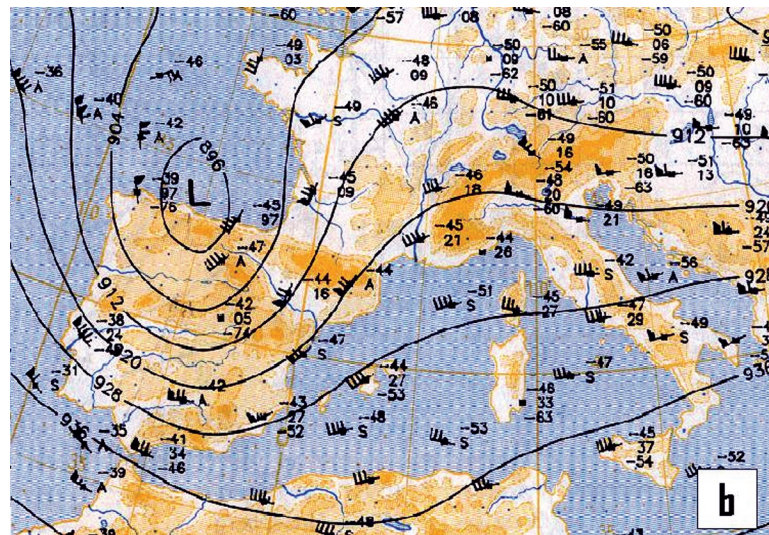
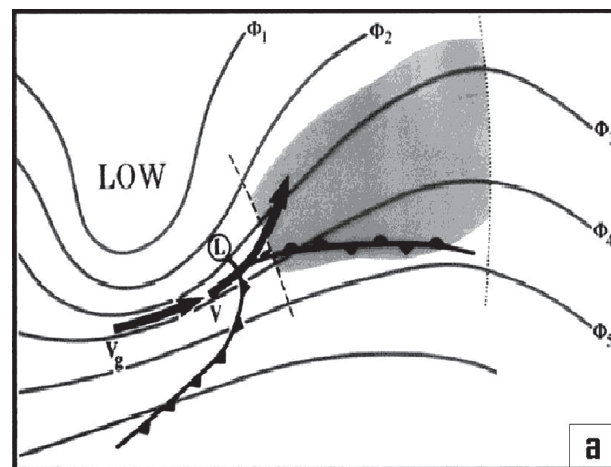


**FIG. 5.** (a) Schematic setting of synoptic environment typifying occurrence of mesoscale gravity waves. Light shading shows the region of wave activity between the axis of inflection and the ridge axis (from Koch and Saleeby 2001). (b) 300-hPa height and wind analysis at 1200 UTC on 20 Oct 1999 (from the DWD European Meteorological Bulletin).

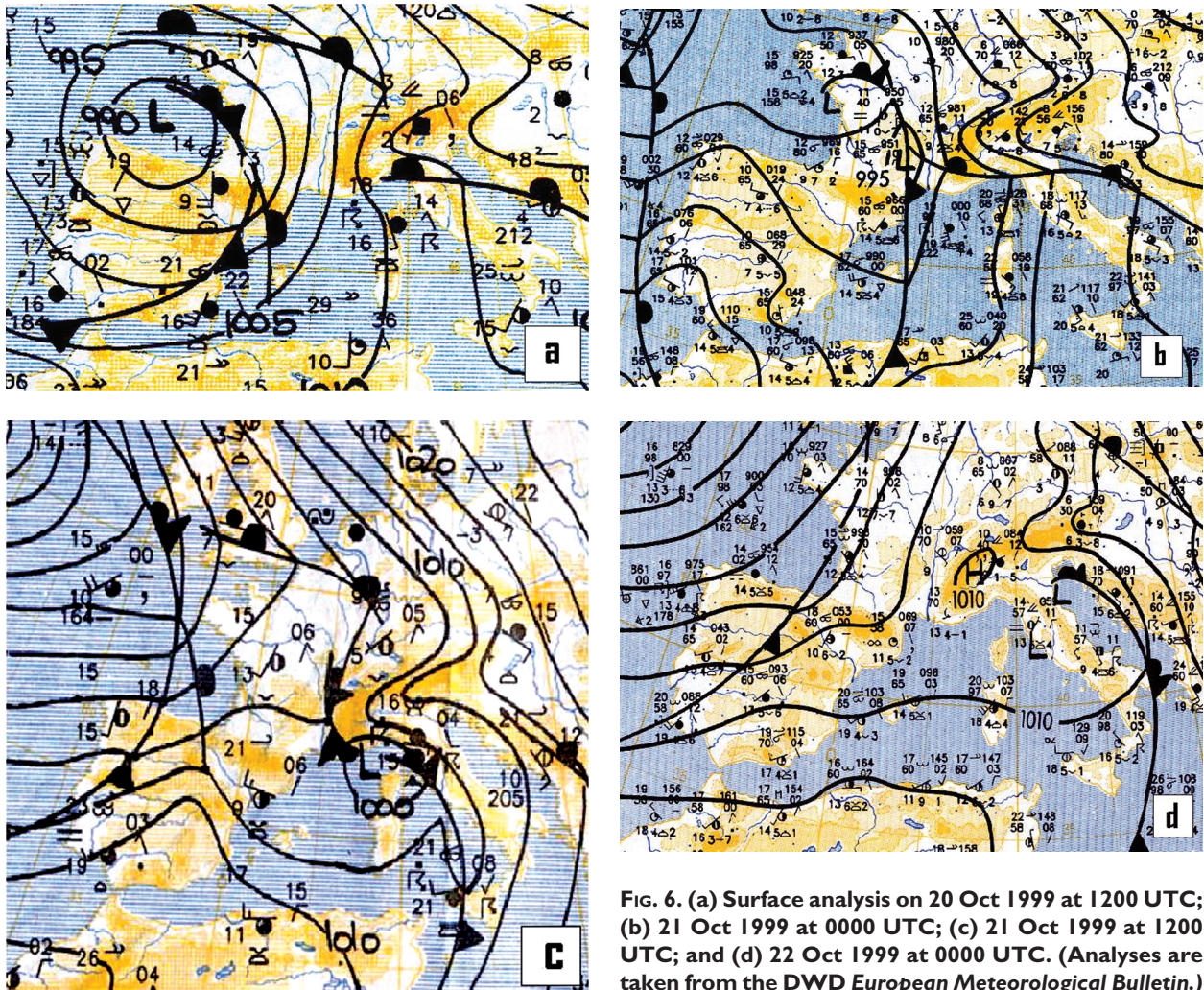


**FIG. 6.** (a) Surface analysis on 20 Oct 1999 at 1200 UTC; (b) 21 Oct 1999 at 0000 UTC; (c) 21 Oct 1999 at 1200 UTC; and (d) 22 Oct 1999 at 0000 UTC. (Analyses are taken from the DWD European Meteorological Bulletin.)

tinuously (Fig. 2). The warm front moved very slowly northeastward, resulting in an occlusion during the morning of 21 October (Fig. 6c). The frontal system progressively weakened and moved toward the Balkan region (Fig. 6d). The rain stopped falling at about 1800 UTC 21 October.

The synoptic situation of this event is typical for heavy precipitation in the western part of the Po valley. When a high ridge in the Balkan region blocks the eastward motion of a system for an extended period of time, severe flooding can happen, such as in the autumn of 1994 and 2000.

On 20 and 21 October 1999, heavy precipitation related to orographic lifting was expected over the southern side of the Alps. However, the high stability in the lower layers limited the lift, and the accumulated precipitation was nearly uniform (below 100 mm) over the slopes and over the valley. At the TRI

station, rainfall reached 52 mm, which was the maximum recorded during the autumn of 1999. The rainfall rate was moderate and strengthened only during the period of the maximum wave activity (0500–1100 UTC on 21 October). During this period, the mean rain rate at TRI was equal to  $0.08 \text{ mm min}^{-1}$ , and the mean amplitude of the periodic variations was equal to  $0.05 \text{ mm min}^{-1}$ . Surface wind records measured 20 km west of TRI showed neither high speeds nor gusts.

In this episode, nearly the entire troposphere was saturated, and in the lowest 3 km the atmosphere was very stable, with an inversion at 2 km (Fig. 3a). The high stability in the Po valley was due to a pool of cold air advected by easterly winds below the inversion (Fig. 3b). The shape of the western Po valley, with the Alps making a barrier to the north and west and the Apennines to the south, represents a real cul de sac for this kind of low-level circulation. This effect was

enhanced by the superimposed westerly–southwesterly (on 20 October) and then southerly (on 21 October) advection of relatively warm, saturated air. The Brunt–Väisälä frequency profile (Fig. 3a) shows a low stability between 3 and 11 km. The atmospheric conditions were therefore favorable for the existence of unstable sheared layers (Richardson number below 0.25) where the flow nearly matched the speed and direction of the wave (Fig. 3b). All the conditions that have been proposed by Uccellini and Koch (1987) seemed therefore fulfilled.

The episode described here was relatively small (pressure amplitudes of 0.4 hPa) and was detected only by employing high-precision microbarometers (0.002 hPa) and a pluviometer (0.01 mm accuracy). Much more severe events can occur, however. Koch and Saleeby (2001) cite the work of Koppel et al. (2000), who compiled a U.S. 25-yr climatology of “gravity-wave events” with amplitudes of at least 4.25 hPa. They calculated an average of 23 such large-amplitude events per year, with the greatest occurrence in cyclonic storm situations peaking between the months of November and April, and those associated with convection peaking in the summer months. These large-amplitude waves can produce wave-normal wind perturbations of  $20 \text{ m s}^{-1}$  and strongly affect the weather.

The gravity-wave events that mostly draw the forecaster’s attention are probably the sequence of severe, multiple thunderstorms that are triggered by mesoscale gravity-wave trains reaching an environment favorable to the formation of strong convection. According to Koch and Saleeby, many of the events listed in Koppel et al. developed in the synoptic environment described by Uccellini and Koch, although they were not necessarily generated by geostrophic adjustment. These phenomena can therefore be forecast with some skill, and Koch and Saleeby have shown that

a forecast can be used to activate a near–real time analysis of the 5-min. observations from the Automated Surface Observing System network. As an example, they analyzed the development of a gravity-wave train that originated in western Kentucky and propagated north–eastward through Ohio in conjunction with banded precipitation. The wave packet had a strong influence upon the surface winds and precipitation fields.

Their analysis demonstrates that the nowcasting of gravity-wave features is becoming more and more a possibility in an operational forecasting environment as the density of the surface observing network and the speed of data access increase. Gravity waves have until now remained primarily a research concern, but the time seems ripe to exploit one of their most important and interesting characteristics: they are generated somewhere by something and, elsewhere, they trigger or influence something else.

## FOR FURTHER READING

- Eom, J. K., 1975: Analysis of the internal gravity wave occurrence of 19 April 1970 in the Midwest. *Mon. Wea. Rev.*, **103**, 217–226.
- Koch, S. E., and S. Saleeby, 2001: An automated system for the analysis of gravity waves and other mesoscale phenomena. *Wea. Forecasting*, **16**, 661–679.
- , and L. M. Siedlarz, 1999: Mesoscale gravity waves and their environment in the central United States during STORM-FEST. *Mon. Wea. Rev.*, **127**, 2854–2879.
- Koppel, L. L., L. F. Bosart, and D. Keyser, 2000: A 25-yr climatology of large-amplitude hourly surface pressure changes over the conterminous United States. *Mon. Wea. Rev.*, **128**, 51–68.
- Uccellini, L. W., and S. E. Koch, 1987: The synoptic setting and possible energy sources for mesoscale wave disturbances. *Mon. Wea. Rev.*, **115**, 721–729.